Draft version August 18, 2022
Typeset using LaTeX **twocolumn** style in AASTeX63

arXiv:2205.09129v2 [astro-ph.GA] 17 Aug 2022

Tucana B: A Potentially Isolated and Quenched Ultra-faint Dwarf Galaxy at D≈1.4 Mpc*

David J. Sand,[1] Burçin Mutlu-Pakdil,[2,3,4] Michael G. Jones,[1] Ananthan Karunakaran,[5] Feige Wang,[1,†] Jinyi Yang,[1,‡] Anirudh Chiti,[2,3] Paul Bennet,[6] Denija Crnojević,[7] and Kristine Spekkens[8,9]

[1]*Steward Observatory, University of Arizona, 933 North Cherry Avenue, Tucson, AZ 85721-0065, USA*
[2]*Kavli Institute for Cosmological Physics, University of Chicago, Chicago, IL 60637, USA*
[3]*Department of Astronomy and Astrophysics, University of Chicago, Chicago IL 60637, USA*
[4]*Department of Physics and Astronomy, Dartmouth College, 6127 Wilder Laboratory, Hanover, NH 03755, USA*
[5]*Instituto de Astrofísica de Andalucía (CSIC), Glorieta de la Astronomía, 18008 Granada, Spain*
[6]*Space Telescope Science Institute, 3700 San Martin Drive, Baltimore, MD 21218, USA*
[7]*University of Tampa, 401 West Kennedy Boulevard, Tampa, FL 33606, USA*
[8]*Department of Physics and Space Science, Royal Military College of Canada, P.O. Box 17000, Station Forces Kingston, ON K7K 7B4, Canada*
[9]*Department of Physics, Engineering Physics and Astronomy, Queen's University, Kingston, ON K7L 3N6, Canada*

(Received; Revised; Accepted)

ABSTRACT

We report the discovery of Tucana B, an isolated ultra-faint dwarf galaxy at a distance of D=1.4 Mpc. Tucana B was found during a search for ultra-faint satellite companions to the known dwarfs in the outskirts of the Local Group, although its sky position and distance indicate the nearest galaxy to be ∼500 kpc distant. Deep ground-based imaging resolves Tucana B into stars, and it displays a sparse red giant branch consistent with an old, metal poor stellar population analogous to that seen in the ultra-faint dwarf galaxies of the Milky Way, albeit at fainter apparent magnitudes. Tucana B has a half-light radius of 80±40 pc, and an absolute magnitude of M_V=$-6.9^{+0.5}_{-0.6}$ mag (L_V=$(5^{+4}_{-2})\times10^4$ $L_\odot$), which is again comparable to the Milky Way's ultra-faint satellites. There is no evidence for a population of young stars, either in the optical color magnitude diagram or in *GALEX* archival ultraviolet imaging, with the *GALEX* data indicating $\log(\mathrm{SFR_{NUV}}/\mathrm{M_\odot\ yr^{-1}}) < -5.4$ for star formation on $\lesssim$100 Myr time scales. Given its isolation and physical properties, Tucana B may be a definitive example of an ultra-faint dwarf that has been quenched by reionization, providing strong confirmation of a key driver of galaxy formation and evolution at the lowest mass scales. It also signals a new era of ultra-faint dwarf galaxy discovery at the extreme edges of the Local Group.

Keywords: Dwarf galaxies (416), Quenched galaxies (2016), Galaxy quenching (2040)

1. INTRODUCTION

The faint end of the galaxy luminosity function is important for understanding dark matter and astrophysics on small scales (see, e.g. Bullock & Boylan-Kolchin 2017; Simon 2019, for recent reviews). In the Local Group, observations continue to find a variety of ultra-faint galaxies (for instance, most recently Mau et al. 2020; Cerny et al. 2021, 2022), while numerical simulations work out how stars form in the smallest dark matter subhalos of Milky Way-like systems (e.g., Brooks et al. 2013; Sawala et al. 2016; Wetzel et al. 2016; Samuel et al. 2020; Engler et al. 2021; Applebaum et al. 2021). Outside of the Local Group, faint dwarf galaxies are being identified in resolved stars (Chiboucas et al. 2013; Sand et al. 2014; Crnojević et al. 2014, 2016b, 2019; Toloba et al. 2016; Carlin et al. 2016; Smercina et al. 2018; Bennet et al. 2019, 2020; Mutlu-Pakdil et al. 2022), diffuse or semi-resolved light (e.g. Bennet et al. 2017; Carlsten et al. 2020; Davis et al. 2021), as well as spectroscopic sur-

Corresponding author: D. J. Sand
dsand@arizona.edu

* This paper includes data gathered with the 6.5 m Magellan Telescope at Las Campanas Observatory, Chile.

† NASA Hubble Fellow

‡ Strittmatter Fellow

veys (Geha et al. 2017; Mao et al. 2021). These programs are leading to a new understanding of both the scatter in satellite properties as well as potential challenges to our picture of galaxy formation on small scales (Bennet et al. 2019, 2020; Carlsten et al. 2021; Smercina et al. 2021; Karunakaran et al. 2021).

Despite this progress, there are still regions of dwarf galaxy discovery space that are largely unexplored. In particular, only a handful of new dwarfs have been uncovered at the periphery of the Local Group and its immediate environs (D≈0.5–2.0 Mpc). Examples include the star forming and relatively isolated dwarf Leo P (D=1.6 Mpc, M_V=−9.3 mag; Giovanelli et al. 2013; Rhode et al. 2013; McQuinn et al. 2015), and the gas-bearing dwarf Antlia B (D=1.35 Mpc, M_V=−9.7 mag; Sand et al. 2015a; Hargis et al. 2020), both of which are members of the NGC 3109 dwarf association. There is also KKR25, an isolated dwarf spheroidal with no signs of recent star formation or neutral gas (D=1.9 Mpc, M_V=−10.9 mag; Makarov et al. 2012). A significant population of faint dwarf galaxies is expected at the edge of the Local Group (e.g. Tollerud & Peek 2018), although recent searches (mostly looking for stellar counterparts to compact, high-velocity H I clouds) have come up short, and only discovered examples of more distant, isolated dwarfs (Adams et al. 2013; Sand et al. 2015b; Bellazzini et al. 2015; Tollerud et al. 2015, 2016; Bennet et al. 2022).

Of particular interest are further examples of quenched dwarf galaxies at the edge of the Local Group. This includes relatively bright objects like Tucana (M_V=−9.5; D=890 kpc) and Cetus (M_V=−11.2; D=700 kpc), which are potential 'backsplash' systems which were plausibly quenched and stripped of their gas after interacting with the Milky Way and have subsequently passed back out of the Local Group (e.g. Teyssier et al. 2012; Buck et al. 2019) – these objects tell us about the orbital evolution of the Milky Way satellite system. Beyond the true edge of the Local Group (∼2-2.5 r_{200}, or ∼750–1000 kpc) it becomes less and less likely that a dwarf galaxy has had a past interaction with the Milky Way (Buck et al. 2019), and it is in this regime where true 'field' dwarfs can be found. Quenched, field dwarfs in the ultra-faint dwarf galaxy regime may cease forming stars not because of any interaction with a larger galaxy, but due to reionization (Babul & Rees 1992; Bullock et al. 2000; Benson et al. 2002; Ricotti & Gnedin 2005; Jeon et al. 2017; Applebaum et al. 2021) or other internal mechanisms, such as supernova feedback (e.g. Dekel & Silk 1986; Mac Low & Ferrara 1999). The discovery of such systems would provide a strong verification of galaxy formation models on small scales.

Here we report the discovery of Tucana B, which to our knowledge is the first quenched, isolated ultra-faint dwarf galaxy identified in the extreme outskirts of the Local Group. The name Tucana B was chosen because of its constellation and the prior existence of the Tucana dwarf spheroidal; a similar naming convention has been used for other dwarfs at the edge of the Local Group (e.g. Sextans A and B; Antlia and Antlia B). We present this new discovery in Section 2, and discuss follow-up optical observations in Section 3. In Section 4 we measure the basic physical properties of Tucana B, and present an analysis of its stellar population. In Section 5 we place Tucana B into context with the satellites of the Milky Way and other dwarfs in the outskirts of the Local Group. In particular, we discuss the environment and isolation of Tucana B, and the ramifications for reionization as a viable quenching mechanism. We summarize and look ahead in Section 6.

2. DISCOVERY OF TUCANA B

Tucana B was found during a visual search for faint dwarf galaxy companions to the distant dwarf spheroidal galaxy Tucana (Lavery & Mighell 1992), at D=890 kpc (Bernard et al. 2009) and M_V=−9.5 (Saviane et al. 1996). To do this, we used data from the DESI Legacy Imaging Surveys Data Release 9 (Dey et al. 2019) and their interactive color image viewer[1]. We uploaded a custom file to mark off a region with projected radius of 100 kpc (≈6.4 deg at the distance of Tucana) and searched for visual over-densities of resolved stars with underlying diffuse light, indicative of a dwarf galaxy at the edge of the Local Group. The field was inspected at a variety of spatial scales and contrast levels.

Tucana B stood out during the search, and is partially resolved into stars in the Legacy Imaging Survey viewer (Figure 1). Tucana B is in the footprint of the Dark Energy Survey Data Release 2 (DES DR2; Abbott et al. 2021), and we downloaded photometry of the field using NOIRLab's Query Interface Tool[2]. Tucana B is not well-resolved in the DES g-band data, but has r and i-band photometry suggestive of a resolved stellar population with an old, metal poor red giant branch (RGB). Given this, we sought deeper ground-based optical data, which we present below.

Tucana B is located ∼6 deg from the Tucana dwarf spheroidal, and is ∼500 kpc more distant along the line of sight (we derive a distance of D=1.4 Mpc to Tu-

[1] https://www.legacysurvey.org/viewer

[2] https://datalab.noirlab.edu/query.php

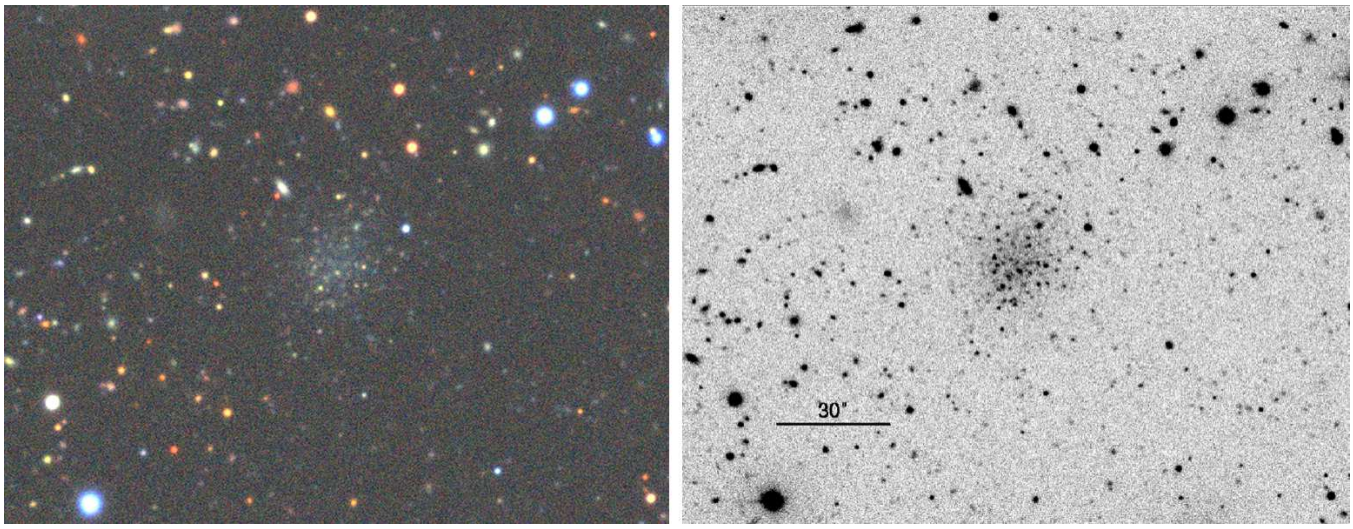


Figure 1. Tucana B as seen in the DESI Legacy Imaging Surveys sky browser (left) and in the deeper Magellan r-band IMACS data (right), where it is more clearly resolved into stars. North is up and East is to the left. The diffuse object to the East of Tucana B is likely a background dwarf galaxy associated with a galaxy group at z=0.036 (Díaz-Giménez & Zandivarez 2015), which is centered to the Northeast and has several other similar, diffuse objects associated with it.

cana B in Section 4.1), and so we provisionally conclude that the two systems are not physically associated. Further, we have performed a careful, final visual search of a 200×200 kpc^2 region centered on Tucana B at our inferred distance and have not identified additional resolved dwarf candidates. We discuss the environment of Tucana B in Section 5.

3. DEEP OPTICAL FOLLOW-UP

Deep g and r-band imaging was taken with the Inamori-Magellan Areal Camera & Spectrograph (IMACS; Dressler et al. 2006) on 2021 Dec 03 (UT). We used the $f/2$ camera, which delivers a ∼27.4′ field of view and 0.2 arcsec/pixel scale. Observations were taken in the g (4×300s) and r (3×300s) bands, with small dithers between exposures. The data were reduced in a standard way (similar to that in Chiti et al. 2020), which included overscan subtraction and flat fielding, followed by an astrometric correction using a combination of ASTROMETRY.NET (Lang et al. 2010) and SCAMP (Bertin 2006). Final image stacking was accomplished with SWARP (Bertin 2010) using a weighted average of the input images. The final g and r band stacked images have point spread function full width half maximum values of 0.8″ and 0.9″, respectively. We display the final, stacked r-band IMACS imaging in the right panel of Figure 1.

We performed point-spread function fitting photometry on the stacked IMACS images, using DAOPHOT and ALLFRAME (Stetson 1987, 1994), following the general procedure described in Mutlu-Pakdil et al. (2018). The photometry was calibrated to point sources in the DES DR2 catalog (Abbott et al. 2021), including a color term, and was corrected for Galactic extinction (Schlafly & Finkbeiner 2011) on a star by star basis. The typical color excess at the position of Tucana B is $E(B-V)$=0.018 mag. In the remainder of this work we present dereddened g_0 and r_0 magnitudes.

To determine our photometric errors and completeness as a function of magnitude and color, we conduct artificial star tests with the DAOPHOT routine ADDSTAR, similar to previous work (Sand et al. 2012; Mutlu-Pakdil et al. 2018). Over several iterations, we injected ∼10^5 artificial stars into our stacked images (a factor of ∼2 more than the number of point sources in the original image) with a range of magnitudes (r=18–29 mag) and colors ($g-r$=−0.5–1.5), and then photometered the simulated data in the same way as the original images. The 50% (90%) completeness level was at r=25.9 (24.5) and g=26.4 (25.1) mag. In Figure 2 we show the color magnitude diagram (CMD) of Tucana B within 1.33 half-light radii r_h (as derived in Section 4.3), along with several equal area "background" CMDs. We discuss the structure and stellar populations of Tucana B in the following section.

4. PROPERTIES OF TUCANA B

In this section we measure the physical properties of Tucana B using our new Magellan photometry, as well as archival H I and *GALEX* UV data sets.

4.1. *Distance*

As we discuss below, the CMD of Tucana B seems to display a stellar population consisting of a sparsely

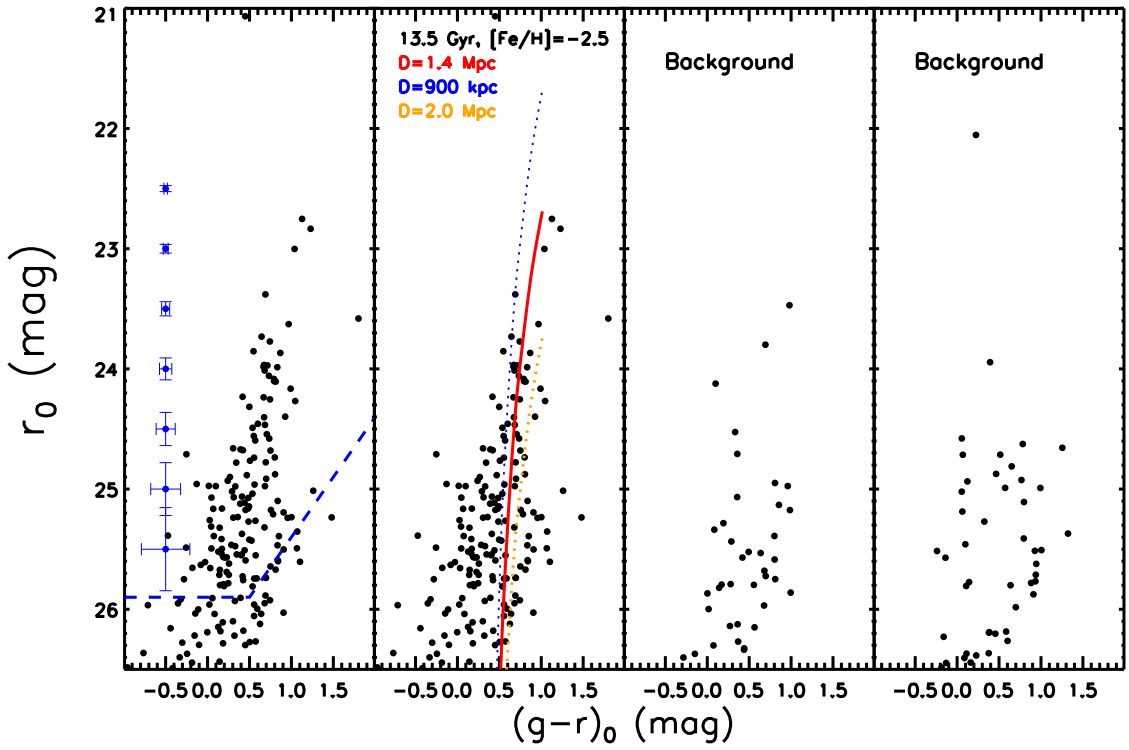


Figure 2. The color-magnitude diagram (CMD) of Tucana B from our Magellan IMACS data (see Section 3). In the two left panels, we display the CMD of Tucana B within 1.33 r_h (16 arcsec). Along the left side of the far-left CMD are the typical uncertainties at different r-band magnitudes, as determined by artificial star tests. The dashed line marks the 50% completeness limit. In the center-left panel we plot 13.5 Gyr, [Fe/H]=−2.5 isochrones (Dotter et al. 2008) at different distances. The blue dotted isochrone is at the distance of the original Tucana dwarf spheroidal (D=900 kpc), while the orange isochrone is at a distance of 2 Mpc. The two panels on the right show randomly selected equal area background regions. There is likely significant background galaxy contamination at $r_0 \gtrsim 24.5$ mag.

Table 1. Tucana B Properties

Parameter	Value
α_0(J2000)	22:47:00.5 ± 1.5"
δ_0(J2000)	−58:24:27.0 ± 2.3"
$m - M$ (mag)	$25.75^{+0.55}_{-0.45}$
Distance (Mpc)	$1.4^{+0.4}_{-0.3}$
M_V (mag)	$-6.9^{+0.5}_{-0.6}$
L_V ($L_\odot$)	$(5^{+4}_{-2})\times10^4$
r_h (arcsec)	12±5
r_h (pc)	80±40
ϵ	<0.35
$\log(\mathrm{SFR_{NUV}}/\mathrm{M_\odot\ yr^{-1}})$	< -5.4
$\log(\mathrm{SFR_{FUV}}/\mathrm{M_\odot\ yr^{-1}})$	< -6.0
$\log(M_{\mathrm{HI}}/M_\odot)$	< 5.6

populated old, metal poor red giant branch (Figure 2). A challenge for measuring the distance to Tucana B is the lack of a well-defined tip of the red giant branch because of its intrinsic faintness, where few or no stars populate the upper regions of the red giant branch, as has been discussed in several previous works (e.g. Madore & Freedman 1995; Weisz et al. 2019; Carlin et al. 2021; Mutlu-Pakdil et al. 2022). The ground-based data are also too shallow to identify a horizontal branch or any associated RR Lyrae stars, both of which could provide distance estimates.

Instead of using a tip of the red giant branch derived distance, we measure the distance to Tucana B using a CMD-fitting technique, comparing the number of stars consistent with several old, metal poor theoretical isochrones, and adopting a methodology similar to that used for several of the Milky Way ultra-faint dwarfs (e.g. Walsh et al. 2008; Sand et al. 2009). We use the Dartmouth isochrones (Dotter et al. 2008), focusing on tracks with stellar ages of 13.5 Gyr and low metallicities ([Fe/H] of −2.5, −2.0 and −1.5). We include all Tucana B stars with r_0<25.5 mag within 0.35′ of its center, which visually encapsulates the bulk of its main

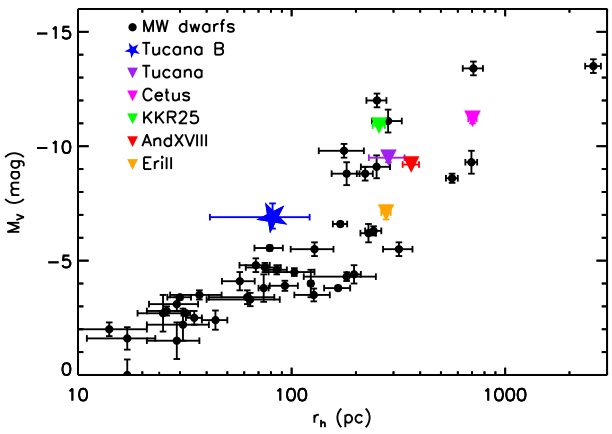


Figure 3. Absolute magnitude as a function of half light radius of Tucana B and other isolated, quenched dwarfs in the outskirts of the Local Group (Cetus: McConnachie & Irwin 2006; Tucana: Saviane et al. 1996; And XVIII: McConnachie et al. 2008; KKR25: Makarov et al. 2012; Eri II: Crnojević et al. 2016a). Also plotted are the dwarf satellites of the Milky Way (McConnachie 2012; Carlin et al. 2017; Muñoz et al. 2018; Mutlu-Pakdil et al. 2018). Tucana B is the faintest and smallest of the isolated, quenched Local Group dwarfs.

body. Each isochrone fiducial is shifted through 0.025 mag intervals in distance modulus ($m-M$) from 24.5 to 27.0 mag (∼0.8–2.5 Mpc). At each of these steps, the number of stars consistent with the fiducial is tabulated. The selection region for stars to be counted is simply defined by two red/blue boundaries in $(g-r)_0$ color for a given r_0 magnitude, as determined by the uncertainties found in our artificial star tests. Background stars are also accounted for by running the identical procedure over an appropriately scaled background region, and then subtracting this number from that of the Tucana B selection. Implicit in this technique is the assumption that Tucana B has a single age, exclusively old (∼13.5 Gyr) stellar population. We have not explored other isochrone model tracks from different groups, or at different ages, which may expand the allowed distance range discussed below. We also assume no internal extinction associated with Tucana B, and only include a Milky Way component.

The best-fit distance moduli for the 13.5 Gyr, [Fe/H]=−2.0 and −2.5 isochrones are $m-M$=25.6 and 25.9 mag (D=1.3 and 1.5 Mpc), respectively. We found the best-fit distance for the 13.5 Gyr, [Fe/H]=−1.5 isochrone unsatisfactory, implying a distance too nearby and too red to properly match the data (see discussion in the next paragraph). Given the two satisfactory matches for a very metal-poor population, we take the mean of those two measurements as our distance modulus ($m-M$=25.75; D=1.4 Mpc), and continue to discuss our uncertainties below.

Given the projected proximity of Tucana B to the original Tucana dwarf spheroidal galaxy, which is at D=900 kpc, we overplot an old metal-poor isochrone (13.5 Gyr, [Fe/H]=−2.5) at that distance onto the CMD in Figure 2. From this, it is clear that Tucana B is at a larger distance than the original Tucana dwarf, otherwise it would imply that the upper 1–2 magnitudes of the red giant branch in Tucana B were completely unpopulated. Thus, the two objects are not likely physically associated, and the lower distance limit to Tucana B is greater than 900 kpc.

As another point of discussion, inspection of the CMD shows three stars at r_0≈22.7–23.0 and $(g-r)_0$≈1.1; the membership status and provenance of these stars is important for assessing the distance of Tucana B. First, aside from our baseline assumption that these stars are upper red giant branch members, these stars may be asymptotic giant branch (AGB) stars associated with Tucana B itself, which would imply that the brightest red giant branch stars are at r_0≈23.5 mag. Alternatively, these stars could be foreground stars, although there are very few contaminant stars at that position in color-magnitude space (see right panels of Figure 2). In either, it may imply a larger distance to Tucana B, although we discount this possibility because it does not match the data. We over plot the same 13.5 Gyr, [Fe/H]=−2.5 isochrone, but at a distance of D=2.0 Mpc, corresponding to a scenario where the three stars at r_0≈22.7–23.0 are either foreground contaminants or AGB stars. While this isochrone roughly matches the putative magnitude of the tip of the red giant branch in this scenario, it is skewed redward of the main locus of Tucana B stars, and cannot be pushed further blueward as it would imply an unrealistically low metallicity for Tucana B. For this reason, Tucana B must be at a closer distance than 2 Mpc, and the three bright aforementioned stars are not likely to be AGB stars or exclusively foreground contaminants.

To determine a distance uncertainty to Tucana B more concrete than the broad limits discussed above, we carefully moved old, metal poor isochrones (both 13.5 Gyr, [Fe/H]=−2 and −2.5) by eye through different distances around our best fit of $m-M$=25.75 (D=1.4 Mpc), and noted where clear departures between isochrone and data occur. For distances much closer than $m-M$=25.75, the isochrones would imply a completely unpopulated upper red giant branch, and the three stars at r_0≈22.7–23.0 become too red to match a metal-poor isochrone. From this inspection we

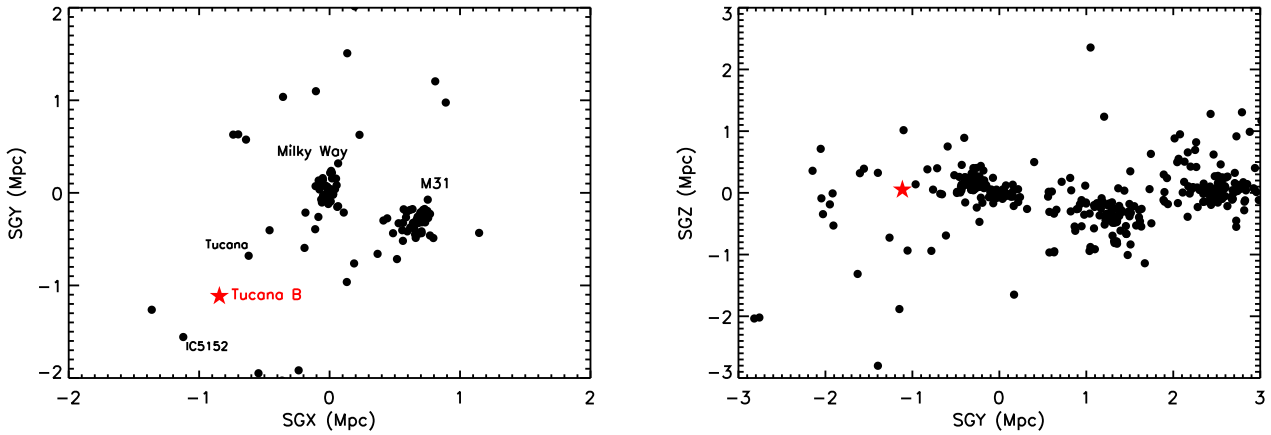


Figure 4. A map of nearby galaxies (from the updated, online version of the Catalog of Neighboring Galaxies; Karachentsev et al. 2004) in supergalactic coordinates, highlighting the isolation of Tucana B. Left: In the supergalactic X-Y plane, looking down on the local plane of galaxies, Tucana B is clearly isolated, with its nearest neighbor being the original Tucana dwarf, at a physical separation of ∼500 kpc. The Large Magellanic Cloud-sized galaxy IC 5152 is separated by ∼620 kpc (at D≈2 Mpc; Karachentsev et al. 2002). These quoted separations are in 3D space, not just in the supergalactic X-Y plane. Right: We show the supergalactic Y-Z plane, which is defined by the local plane of galaxies, used to roughly define the supergalactic coordinate system.

estimate a lower distance limit of $m-M$=25.3 (D=1.1 Mpc). For distances farther than $m-M$=25.75, we were most concerned about the isochrone skewing redwards of the data, without much concern for the three stars at r_0≈22.7–23.0 as these may be contaminants or member AGB stars in this scenario, as discussed above. This leads to a visual upper distance limit of $m-M$=26.3 (D=1.8 Mpc). While we emphasize that space-based data down to the horizontal branch is necessary for a definitive distance to Tucana B, the ground-based CMD indicates a $m-M=25.75^{+0.55}_{-0.45}$ mag ($D=1.4^{+0.4}_{-0.3}$ Mpc).

4.2. *Stellar Population*

Based on the CMD and our distance constraints, Tucana B appears to only consist of an old metal-poor stellar population (Figure 2). Other recently discovered dwarfs at the edge of the Local Group, such as Leo P ($M_V=-9.3$) and Antlia B ($M_V=-9.7$), have clear signs of star formation in the form of blue main sequence stars (McQuinn et al. 2015; Hargis et al. 2020), but any plausible blue member stars in Tucana B are small in number and consistent with background contamination (Figure 2). Its CMD is most analogous to the ultra-faint dwarf galaxies of the Milky Way, which only consist of an old stellar population, with the exception of Leo T (de Jong et al. 2008; Weisz et al. 2012).

To further assess any possible young stellar population, we search for coincident UV emission with data from the *Galaxy Evolution Explorer* (*GALEX*; Martin et al. 2005) archive, which is sensitive to star formation on $\lesssim$100 Myr time scales (e.g. Lee et al. 2011). We adopt the methodology of Karunakaran et al. (2021), using a 16 arcsec aperture ($1.33r_h$), finding no detection at the position of Tucana B. We assess our detection limits by placing 1000 random apertures over the *GALEX* field (after masking bright objects). We then translate these NUV and FUV flux limits to star formation rate limits using the relations of Iglesias-Páramo et al. (2006), finding $\log(\mathrm{SFR_{NUV}}/\mathrm{M_\odot\,yr^{-1}}) < -5.4$ and $\log(\mathrm{SFR_{FUV}}/\mathrm{M_\odot\,yr^{-1}}) < -6.0$, respectively. Both limits are more than an order of magnitude more stringent than nearly all UV detections in satellite galaxies around Milky Way-like halos (e.g. Karunakaran et al. 2021), again emphasizing the lack of star formation in Tucana B.

It is important to note that the current data set cannot rule out the presence of a faint intermediate age stellar population, greater than ∼500 Myr old. Such intermediate age stellar populations do exist in faint dwarf galaxies in the Local Group, for instance in the *HST* imaging of Andromeda XVI (Weisz et al. 2014b). To be sensitive to such stellar populations will require deep space-based observations, as we continue to emphasize in this work.

4.3. *Stellar Structure and Luminosity*

Tucana B is a distant stellar system with only ∼100 resolved stars in our Magellan/IMACS data. As in previous work on similarly sparse systems (e.g. Sand et al. 2014), we fit an exponential profile to the two-dimensional distribution of stars consistent with the red giant branch of Tucana B using the maximum likeli-

hood technique of Martin et al. (2008). We select stars for this analysis which are consistent with the best-fitting Dartmouth isochrone, at a distance of D =1.4 Mpc as found in Section 4.1, after taking into account the photometric uncertainties for stars brighter than the 50% completeness limit. The fit includes the central position (α_0,δ_0), position angle (θ), ellipticity (ϵ), half-light radius (r_h), and a constant background surface density as free parameters. Uncertainties on each parameter were calculated through a bootstrap resampling analysis, with 1000 iterations. As a check on our results, we repeated the calculations while only including red giant branch stars down to r_0=25.4 mag, a half magnitude brighter than our initial iteration; the derived structural parameters did not change to within the uncertainties.

The results of the structural analysis are shown in Table 1. Tucana B has a half light radius of 80±40 pc (this includes our distance uncertainty). Its ellipticity is not well-constrained: we find an upper limit of <0.35 at 95% confidence, reinforcing the roughly circular shape of the dwarf seen in Figure 1. Given this, no constraint on the position angle is possible. The central position of the new dwarf is constrained to a couple of arcseconds.

To derive the luminosity of Tucana B we employ the methodology of Martin et al. (2008), which is appropriate for faint dwarf galaxies in the 'CMD shot noise' regime, where the presence or absence of individual stars in the upper RGB can greatly influence the overall luminosity. First, we build a well-populated CMD by using a [Fe/H]=−2, 13.5 Gyr isochrone and a Salpeter initial mass function. We convolve this with our measured completeness and photometric uncertainties, shifted to D = 1.4 Mpc. We then randomly selected the same number of stars from the simulated CMD as was found in our maximum likelihood analysis, taking into account the luminosity in the simulated population below our detection limit. We repeat this process 100 times, taking the median and standard deviation as our final absolute magnitude and uncertainty (we also add the distance uncertainty in quadrature for our final absolute magnitude uncertainty). We convert to the V-band using the filter transformation equations of Jordi et al. (2006), and ultimately find $M_V=-6.9^{+0.5}_{-0.6}$ mag ($L_V=(5^{+4}_{-2})\times10^4$ $L_\odot$). Based on this, Tucana B is a true ultra-faint dwarf galaxy, similar in luminosity to Eridanus II (Crnojević et al. 2016a).

4.4. *Gas Content*

Given the isolation and apparent lack of recent star formation in Tucana B, it is important to assess its neutral gas content. The deepest available H I observations in the direction of Tucana B are from the Galactic All Sky Survey (GASS; McClure-Griffiths et al. 2009; Kalberla et al. 2010; Kalberla & Haud 2015), with the caveat that these observations only extend to a redshift of ∼500 km s^{-1}. Tucana B is located in a field surrounded by complex foreground H I features associated with the Milky Way and Magellanic Clouds (e.g. Westmeier 2018). This complicates the search for an H I counterpart of Tucana B as, without an a priori redshift, any H I emission along the line-of-sight could be associated with the Milky Way. Although difficult, it will be important to measure a stellar velocity for Tucana B for this task.

In the GASS data there is a clump of H I emission that peaks approximately 20′ to the SW of Tucana B (note that the spatial resolution of the GASS data is 16′). This clump (at $cz_\odot \approx 220$ km s^{-1}) forms a distinct, almost point-like (at the resolution of GASS) feature, but is surrounded by Milky Way emission. Therefore, it is highly likely that this feature is merely associated with the Milky Way and not Tucana B, but we cannot robustly exclude either option with the available data.

There is no other candidate feature in the GASS data, therefore, if we assume this feature is not associated with Tucana B then we can proceed to set an upper limit on its H I mass. The typical rms noise of GASS is 53 mK in 0.82 km s^{-1} channels. Approximating the Parkes radio telescope gain as 0.7 K/Jy gives a 3σ sensitivity of $\log(M_{\rm HI}/M_\odot) < 5.6$ for a source of 20 km s^{-1} velocity width and a distance of 1.4 Mpc. Future high-resolution, interferometric observations, potentially with MeerKAT or the Australia Telescope Compact Array (ATCA) are necessary to further constrain the HI content of Tucana B.

5. DISCUSSION

Tucana B is a unique discovery for a dwarf galaxy just beyond the Local Group, given both its luminosity, isolation and its lack of apparent star formation or neutral gas. Here we discuss the physical properties and environment of Tucana B in the broader context of faint dwarf galaxies as a population.

5.1. *Local Group and Isolated Dwarf Comparisons*

In Figure 3 we plot a size – luminosity relation featuring the satellites of the Milky Way, along with quenched dwarfs in the outskirts of the Local Group. We also highlight Eridanus II, which is situated near the virial radius of the Milky Way itself, but is devoid of recent star formation and gas.

In comparison to the Milky Way satellites, Tucana B has a luminosity similar to Eridanus II (Crnojević et al. 2016a; Simon et al. 2021), and is slightly more luminous than the ultra-faint dwarfs Boötes I (M_V=−6.0

mag; Muñoz et al. 2018) and Hercules (M_V=−6.2 mag; Sand et al. 2009). Interestingly, Tucana B is significantly more compact than either of these systems, which have half light radii $\gtrsim$200 pc. Its half light radius is comparable to much fainter satellites such as Canes Venatici II ($M_V\approx-4.6$ mag; $r_h\approx$85 pc; Sand et al. 2012).

Despite its compact nature for its luminosity, Tucana B is only a mild outlier in comparison to the Milky Way dwarf population as a whole, especially considering its large uncertainties. If a larger population of field ultra-faint dwarfs display a more compact stellar distribution than their counterparts near the Milky Way, it may point to dwarf mergers, tidal encounters or similar mechanisms puffing up the stellar distribution in the Milky Way sample (e.g. Frings et al. 2017; Chiti et al. 2021; Tarumi et al. 2021), although this is just speculation at this point.

5.2. *Environment*

To investigate the environment of Tucana B, we plot the known dwarfs and galaxies of the Local Volume in two projections of the supergalactic coordinate system in Figure 4. We focus on the supergalactic X-Y projection, as the Y-Z plot simply shows the local plane of galaxies used to roughly define the supergalactic coordinate system; note that Tucana B is on this plane. Given our search area, it is no surprise that the nearest galaxy to Tucana B is the original Tucana dwarf, at a physical separation of ∼500 kpc, followed by the low-mass galaxy IC5152 (∼620 kpc separation). Both of these separations are beyond the virial radius of either low-mass galaxy (even with the considerable Tucana B distance uncertainties). As mentioned elsewhere, it will be important to measure a velocity to Tucana B to further assess whether it interacted with either low mass system in the past. Tucana B is also well beyond the virial radius of the Milky Way itself, which is between r_{vir}=200–300 kpc (e.g. Klypin et al. 2002; Putman et al. 2021), putting it at $\gtrsim$4.5 r_{vir}. Barring future discoveries, Tucana B is one of the most isolated galaxies within ∼2 Mpc.

5.3. *The Nature of Tucana B*

Tucana B is an apparently quenched, isolated ultra-faint dwarf galaxy which may have deep implications for our view of low mass galaxy formation, depending on its origins.

First, it is possible that Tucana B is a so-called backsplash galaxy, and may have had a previous encounter with the Milky Way, quenching its star formation and stripping it of its gas before being ejected out to large galactocentric radii. Several systems in the outskirts of the Local Group have been identified as possible backsplash systems (see, for instance, Table 4 in Buck et al. 2019, for one sample). In order to fully assess this scenario, a velocity measurement of Tucana B is necessary, and both a stellar velocity measurement and deeper H I observations should be prioritized. Nonetheless, simulations suggest it is very unlikely that Tucana B is a backsplash system, as most such galaxies should be at $\lesssim$2.5 r_{vir} (e.g. Teyssier et al. 2012; Diemer & Kravtsov 2015; Buck et al. 2019; Applebaum et al. 2021), which is significantly closer to the Milky Way than Tucana B.

It is also possible that Tucana B is a faint example of a transition dwarf galaxy, which exhibit HI emission, but show no signs of recent star formation (Skillman et al. 2003; Weisz et al. 2011), possibly because they are in between star formation episodes (see e.g. El-Badry et al. 2016). While no HI emission is detected in Tucana B, more stringent limits are necessary to rule out this scenario (preferably down to $M_{HI}/L_V\approx1$; e.g. Putman et al. 2021), along with deeper photometry to probe intermediate age star formation events.

As the backsplash scenario is unlikely, it points to Tucana B being a true quenched field ultra-faint dwarf galaxy (again with the caveat that deeper optical and H I data are necessary). Without any interaction with the hot halo or gravitational field of a massive galaxy, reionization and/or some other internal mechanism (i.e. supernova feedback) is likely responsible for the gas free and quenched status of Tucana B. Such a scenario is seen in recent simulations of field dwarf galaxies (e.g. Jeon et al. 2017; Rey et al. 2020; Applebaum et al. 2021), although even here it is possible for faint dwarf galaxies to be quenched by other mechanisms, such as ram pressure stripping by gas in the cosmic web itself (e.g. Benítez-Llambay et al. 2013).

It has long been recognized that reionization can essentially 'boil' the gas out of the dark matter potential wells of ultra-faint dwarf galaxies, explaining their dearth of stars and the possibility that some dark matter halos never form stars at all (e.g. Babul & Rees 1992; Bullock et al. 2000; Benson et al. 2002; Ricotti & Gnedin 2005). Observations of the ultra-faint dwarfs around the Milky Way lend support to this picture, as *HST* observations down to the oldest main sequence turnoff reveal nearly synchronous star formation at very early times (∼13 Gyr ago), with little to no star formation since the reionization epoch (Brown et al. 2014; Weisz et al. 2014a). However, as the Milky Way ultra-faint dwarfs have also experienced its hot halo and significant tidal forces, it is difficult to distinguish between all of these mechanisms as the pri-

mary source for their quenched, gas-free status. Thus, Tucana B may provide strong confirmation of reionization's role in influencing galaxy formation and evolution at the lowest mass scales.

6. SUMMARY & FUTURE OUTLOOK

We have presented the discovery of Tucana B, an ultra-faint dwarf galaxy in the extreme outskirts of the Local Group ($D\approx$1.4 Mpc). Its luminosity ($M_V=-6.9$ mag) and apparent lack of star formation and neutral gas make it unique among recent discoveries at this approximate distance (e.g. Makarov et al. 2012; Giovanelli et al. 2013; Sand et al. 2015a). The isolation of Tucana B also suggests that its star formation was quenched by reionization or some other internal mechanism, rather than interaction with a larger galaxy halo, although further data is necessary to solidify these results. Even if it is found that Tucana B has an intermediate age stellar population, or contained a reservoir of HI gas, it will still be a novel ultra-faint dwarf with properties distinct from those found around the Milky Way. It is likely that similar systems to Tucana B are waiting to be discovered, although its semi-resolved status in the discovery DECam data point to the need for a tailored search. A complete census of such objects is necessary to understand the demographics of the field ultra-faint dwarf galaxy population.

Tucana B is a prime target for future space-based follow-up to pin down its structure and star formation history, possibly down to the oldest main sequence turnoff. In particular, Tucana B may provide a definitive opportunity to understand the role that reionization plays in the quenching of the faintest galaxies. As discussed, *HST* observations of the Milky Way's ultra-faint dwarfs down to the oldest main sequence turnoff reveal early, nearly synchronous star formation (Brown et al. 2014; Weisz et al. 2014a). There are hints that those ultra-faint dwarfs associated with the Magellanic Clouds had a slightly different star formation epoch than those of the Milky Way (Sacchi et al. 2021), and probing further systems and environments is essential for confirming and extending these results. Prior to the advent of the *James Webb Space Telescope*, similar observations beyond the Local Group were prohibitive, but the Near Infrared Camera (NIRCam) enables such studies out to $\sim$2 Mpc (e.g. Weisz & Boylan-Kolchin 2019). Tucana B, and similar systems to be discovered in the near-future (e.g. see predictions and simulated data in Rodriguez Wimberly et al. 2019; Mutlu-Pakdil et al. 2021, respectively), will be a crucial data set for understanding reionization's effect on star formation and subsequent cessation in the smallest dark matter halos.

ACKNOWLEDGMENTS

DJS acknowledges support from NSF grants AST-1821967 and 1813708. BMP is supported by an NSF Astronomy and Astrophysics Postdoctoral Fellowship under award AST-2001663. Research by DC is supported by NSF grant AST-1814208. AK acknowledges financial support from the State Agency for Research of the Spanish Ministry of Science, Innovation and Universities through the "Center of Excellence Severo Ochoa" awarded to the Instituto de Astrofísica de Andalucía (SEV-2017-0709) and through the grant POST-DOC_21_00845 financed from the budgetary program 54a Scientific Research and Innovation of the Economic Transformation, Industry, Knowledge and Universities Council of the Regional Government of Andalusia. F.W. thanks the support provided by NASA through the NASA Hubble Fellowship grant #HF2-51448 awarded by the Space Telescope Science Institute, which is operated by the Association of Universities for Research in Astronomy, Incorporated, under NASA contract NAS5-26555. AC is supported by a Brinson Prize Fellowship at UChicago/KICP. KS acknowledges support from the Natural Sciences and Engineering Research Council of Canada (NSERC).

This research uses services or data provided by the Astro Data Lab at NSF's National Optical-Infrared Astronomy Research Laboratory. NOIRLab is operated by the Association of Universities for Research in Astronomy (AURA), Inc. under a cooperative agreement with the National Science Foundation.

The work used images from the Dark Energy Camera Legacy Survey (DECaLS; Proposal ID 2014B-0404; PIs: David Schlegel and Arjun Dey). Full acknowledgment at https://www.legacysurvey.org/acknowledgment/.

This research is based on observations made with the *Galaxy Evolution Explorer*, obtained from the MAST data archive at the Space Telescope Science Institute, which is operated by the Association of Universities for Research in Astronomy, Inc., under NASA contract NAS 5–26555.

This project used public archival data from the Dark Energy Survey (DES). Funding for the DES Projects has been provided by the U.S. Department of Energy, the U.S. National Science Foundation, the Ministry of Science and Education of Spain, the Science and Technology Facilities Council of the United Kingdom, the Higher Education Funding Council for England, the National Center for Supercomputing Applications at the University of Illinois at Urbana-Champaign, the Kavli Institute of Cosmological Physics at the University of Chicago, the Center for Cosmology and Astro-Particle

Physics at the Ohio State University, the Mitchell Institute for Fundamental Physics and Astronomy at Texas A&M University, Financiadora de Estudos e Projetos, Fundação Carlos Chagas Filho de Amparo à Pesquisa do Estado do Rio de Janeiro, Conselho Nacional de Desenvolvimento Científico e Tecnológico and the Ministério da Ciência, Tecnologia e Inovação, the Deutsche Forschungsgemeinschaft, and the Collaborating Institutions in the Dark Energy Survey. The Collaborating Institutions are Argonne National Laboratory, the University of California at Santa Cruz, the University of Cambridge, Centro de Investigaciones Energéticas, Medioambientales y Tecnológicas-Madrid, the University of Chicago, University College London, the DES-Brazil Consortium, the University of Edinburgh, the Eidgenössische Technische Hochschule (ETH) Zürich, Fermi National Accelerator Laboratory, the University of Illinois at Urbana-Champaign, the Institut de Ciències de l'Espai (IEEC/CSIC), the Institut de Física d'Altes Energies, Lawrence Berkeley National Laboratory, the Ludwig-Maximilians Universität München and the associated Excellence Cluster Universe, the University of Michigan, the National Optical Astronomy Observatory, the University of Nottingham, The Ohio State University, the OzDES Membership Consortium, the University of Pennsylvania, the University of Portsmouth, SLAC National Accelerator Laboratory, Stanford University, the University of Sussex, and Texas A&M University. Based in part on observations at Cerro Tololo Inter-American Observatory, National Optical Astronomy Observatory, which is operated by the Association of Universities for Research in Astronomy (AURA) under a cooperative agreement with the National Science Foundation.

Facilities: Magellan:Baade (IMACS), *GALEX*, Parkes, Blanco

Software: astropy (Astropy Collaboration et al. 2013; The Astropy Collaboration et al. 2018), ASTROMETRY.NET (Lang et al. 2010) The IDL Astronomy User's Library (Landsman 1993), DAOPHOT (Stetson 1987, 1994), SCAMP (Bertin 2006), SWARP (Bertin 2010)

REFERENCES

Abbott, T. M. C., Adamów, M., Aguena, M., et al. 2021, ApJS, 255, 20, doi: 10.3847/1538-4365/ac00b3

Adams, E. A. K., Giovanelli, R., & Haynes, M. P. 2013, ApJ, 768, 77, doi: 10.1088/0004-637X/768/1/77

Applebaum, E., Brooks, A. M., Christensen, C. R., et al. 2021, ApJ, 906, 96, doi: 10.3847/1538-4357/abcafa

Astropy Collaboration, Robitaille, T. P., Tollerud, E. J., et al. 2013, A&A, 558, A33, doi: 10.1051/0004-6361/201322068

Babul, A., & Rees, M. J. 1992, MNRAS, 255, 346, doi: 10.1093/mnras/255.2.346

Bellazzini, M., Beccari, G., Battaglia, G., et al. 2015, A&A, 575, A126, doi: 10.1051/0004-6361/201425262

Benítez-Llambay, A., Navarro, J. F., Abadi, M. G., et al. 2013, ApJL, 763, L41, doi: 10.1088/2041-8205/763/2/L41

Bennet, P., Sand, D. J., Crnojević, D., et al. 2019, ApJ, 885, 153, doi: 10.3847/1538-4357/ab46ab

—. 2020, ApJL, 893, L9, doi: 10.3847/2041-8213/ab80c5

—. 2017, ApJ, 850, 109, doi: 10.3847/1538-4357/aa9180

—. 2022, ApJ, 924, 98, doi: 10.3847/1538-4357/ac356c

Benson, A. J., Frenk, C. S., Lacey, C. G., Baugh, C. M., & Cole, S. 2002, MNRAS, 333, 177, doi: 10.1046/j.1365-8711.2002.05388.x

Bernard, E. J., Monelli, M., Gallart, C., et al. 2009, ApJ, 699, 1742, doi: 10.1088/0004-637X/699/2/1742

Bertin, E. 2006, in Astronomical Society of the Pacific Conference Series, Vol. 351, Astronomical Data Analysis Software and Systems XV, ed. C. Gabriel, C. Arviset, D. Ponz, & S. Enrique, 112

Bertin, E. 2010, SWarp: Resampling and Co-adding FITS Images Together. http://ascl.net/1010.068

Brooks, A. M., Kuhlen, M., Zolotov, A., & Hooper, D. 2013, ApJ, 765, 22, doi: 10.1088/0004-637X/765/1/22

Brown, T. M., Tumlinson, J., Geha, M., et al. 2014, ApJ, 796, 91, doi: 10.1088/0004-637X/796/2/91

Buck, T., Macciò, A. V., Dutton, A. A., Obreja, A., & Frings, J. 2019, MNRAS, 483, 1314, doi: 10.1093/mnras/sty2913

Bullock, J. S., & Boylan-Kolchin, M. 2017, ARA&A, 55, 343, doi: 10.1146/annurev-astro-091916-055313

Bullock, J. S., Kravtsov, A. V., & Weinberg, D. H. 2000, ApJ, 539, 517, doi: 10.1086/309279

Carlin, J. L., Sand, D. J., Price, P., et al. 2016, ApJL, 828, L5, doi: 10.3847/2041-8205/828/1/L5

Carlin, J. L., Sand, D. J., Muñoz, R. R., et al. 2017, AJ, 154, 267, doi: 10.3847/1538-3881/aa94d0

Carlin, J. L., Mutlu-Pakdil, B., Crnojević, D., et al. 2021, ApJ, 909, 211, doi: 10.3847/1538-4357/abe040

Carlsten, S. G., Greco, J. P., Beaton, R. L., & Greene, J. E. 2020, ApJ, 891, 144, doi: 10.3847/1538-4357/ab7758

Carlsten, S. G., Greene, J. E., Peter, A. H. G., Beaton, R. L., & Greco, J. P. 2021, ApJ, 908, 109, doi: 10.3847/1538-4357/abd039

Cerny, W., Pace, A. B., Drlica-Wagner, A., et al. 2021, ApJL, 920, L44, doi: 10.3847/2041-8213/ac2d9a

Cerny, W., Simon, J. D., Li, T. S., et al. 2022, arXiv e-prints, arXiv:2203.11788. https://arxiv.org/abs/2203.11788

Chiboucas, K., Jacobs, B. A., Tully, R. B., & Karachentsev, I. D. 2013, AJ, 146, 126, doi: 10.1088/0004-6256/146/5/126

Chiti, A., Frebel, A., Jerjen, H., Kim, D., & Norris, J. E. 2020, ApJ, 891, 8, doi: 10.3847/1538-4357/ab6d72

Chiti, A., Frebel, A., Simon, J. D., et al. 2021, Nature Astronomy, 5, 392, doi: 10.1038/s41550-020-01285-w

Crnojević, D., Sand, D. J., Zaritsky, D., et al. 2016a, ApJL, 824, L14, doi: 10.3847/2041-8205/824/1/L14

Crnojević, D., Sand, D. J., Caldwell, N., et al. 2014, ApJL, 795, L35, doi: 10.1088/2041-8205/795/2/L35

Crnojević, D., Sand, D. J., Spekkens, K., et al. 2016b, ApJ, 823, 19, doi: 10.3847/0004-637X/823/1/19

Crnojević, D., Sand, D. J., Bennet, P., et al. 2019, ApJ, 872, 80, doi: 10.3847/1538-4357/aafbe7

Davis, A. B., Nierenberg, A. M., Peter, A. H. G., et al. 2021, MNRAS, 500, 3854, doi: 10.1093/mnras/staa3246

de Jong, J. T. A., Harris, J., Coleman, M. G., et al. 2008, ApJ, 680, 1112, doi: 10.1086/587835

Dekel, A., & Silk, J. 1986, ApJ, 303, 39, doi: 10.1086/164050

Dey, A., Schlegel, D. J., Lang, D., et al. 2019, AJ, 157, 168, doi: 10.3847/1538-3881/ab089d

Díaz-Giménez, E., & Zandivarez, A. 2015, A&A, 578, A61, doi: 10.1051/0004-6361/201425267

Diemer, B., & Kravtsov, A. V. 2015, ApJ, 799, 108, doi: 10.1088/0004-637X/799/1/108

Dotter, A., Chaboyer, B., Jevremović, D., et al. 2008, ApJS, 178, 89, doi: 10.1086/589654

Dressler, A., Hare, T., Bigelow, B. C., & Osip, D. J. 2006, in Society of Photo-Optical Instrumentation Engineers (SPIE) Conference Series, Vol. 6269, Society of Photo-Optical Instrumentation Engineers (SPIE) Conference Series, ed. I. S. McLean & M. Iye, 62690F, doi: 10.1117/12.670573

El-Badry, K., Wetzel, A., Geha, M., et al. 2016, ApJ, 820, 131, doi: 10.3847/0004-637X/820/2/131

Engler, C., Pillepich, A., Pasquali, A., et al. 2021, arXiv e-prints, arXiv:2101.12215. https://arxiv.org/abs/2101.12215

Frings, J., Macciò, A., Buck, T., et al. 2017, MNRAS, 472, 3378, doi: 10.1093/mnras/stx2171

Geha, M., Wechsler, R. H., Mao, Y.-Y., et al. 2017, ApJ, 847, 4, doi: 10.3847/1538-4357/aa8626

Giovanelli, R., Haynes, M. P., Adams, E. A. K., et al. 2013, AJ, 146, 15, doi: 10.1088/0004-6256/146/1/15

Hargis, J. R., Albers, S., Crnojević, D., et al. 2020, ApJ, 888, 31, doi: 10.3847/1538-4357/ab58d2

Iglesias-Páramo, J., Buat, V., Takeuchi, T. T., et al. 2006, ApJS, 164, 38, doi: 10.1086/502628

Jeon, M., Besla, G., & Bromm, V. 2017, ApJ, 848, 85, doi: 10.3847/1538-4357/aa8c80

Jordi, K., Grebel, E. K., & Ammon, K. 2006, A&A, 460, 339, doi: 10.1051/0004-6361:20066082

Kalberla, P. M. W., & Haud, U. 2015, A&A, 578, A78, doi: 10.1051/0004-6361/201525859

Kalberla, P. M. W., McClure-Griffiths, N. M., Pisano, D. J., et al. 2010, A&A, 521, A17, doi: 10.1051/0004-6361/200913979

Karachentsev, I. D., Karachentseva, V. E., Huchtmeier, W. K., & Makarov, D. I. 2004, AJ, 127, 2031, doi: 10.1086/382905

Karachentsev, I. D., Sharina, M. E., Makarov, D. I., et al. 2002, A&A, 389, 812, doi: 10.1051/0004-6361:20020649

Karunakaran, A., Spekkens, K., Oman, K. A., et al. 2021, ApJL, 916, L19, doi: 10.3847/2041-8213/ac0e3a

Klypin, A., Zhao, H., & Somerville, R. S. 2002, ApJ, 573, 597, doi: 10.1086/340656

Landsman, W. B. 1993, in Astronomical Society of the Pacific Conference Series, Vol. 52, Astronomical Data Analysis Software and Systems II, ed. R. J. Hanisch, R. J. V. Brissenden, & J. Barnes, 246

Lang, D., Hogg, D. W., Mierle, K., Blanton, M., & Roweis, S. 2010, AJ, 139, 1782, doi: 10.1088/0004-6256/139/5/1782

Lavery, R. J., & Mighell, K. J. 1992, AJ, 103, 81, doi: 10.1086/116042

Lee, J. C., Gil de Paz, A., Kennicutt, Robert C., J., et al. 2011, ApJS, 192, 6, doi: 10.1088/0067-0049/192/1/6

Mac Low, M.-M., & Ferrara, A. 1999, ApJ, 513, 142, doi: 10.1086/306832

Madore, B. F., & Freedman, W. L. 1995, AJ, 109, 1645, doi: 10.1086/117391

Makarov, D., Makarova, L., Sharina, M., et al. 2012, MNRAS, 425, 709, doi: 10.1111/j.1365-2966.2012.21581.x

Mao, Y.-Y., Geha, M., Wechsler, R. H., et al. 2021, ApJ, 907, 85, doi: 10.3847/1538-4357/abce58

Martin, D. C., Fanson, J., Schiminovich, D., et al. 2005, ApJL, 619, L1, doi: 10.1086/426387

Martin, N. F., de Jong, J. T. A., & Rix, H.-W. 2008, ApJ, 684, 1075, doi: 10.1086/590336

Mau, S., Cerny, W., Pace, A. B., et al. 2020, ApJ, 890, 136, doi: 10.3847/1538-4357/ab6c67
McClure-Griffiths, N. M., Pisano, D. J., Calabretta, M. R., et al. 2009, ApJS, 181, 398, doi: 10.1088/0067-0049/181/2/398
McConnachie, A. W. 2012, AJ, 144, 4, doi: 10.1088/0004-6256/144/1/4
McConnachie, A. W., & Irwin, M. J. 2006, MNRAS, 365, 1263, doi: 10.1111/j.1365-2966.2005.09806.x
McConnachie, A. W., Huxor, A., Martin, N. F., et al. 2008, ApJ, 688, 1009, doi: 10.1086/591313
McQuinn, K. B. W., Skillman, E. D., Dolphin, A., et al. 2015, ApJ, 812, 158, doi: 10.1088/0004-637X/812/2/158
Muñoz, R. R., Côté, P., Santana, F. A., et al. 2018, ApJ, 860, 66, doi: 10.3847/1538-4357/aac16b
Mutlu-Pakdil, B., Sand, D. J., Carlin, J. L., et al. 2018, ApJ, 863, 25, doi: 10.3847/1538-4357/aacd0e
Mutlu-Pakdil, B., Sand, D. J., Crnojević, D., et al. 2021, ApJ, 918, 88, doi: 10.3847/1538-4357/ac0db8
—. 2022, ApJ, 926, 77, doi: 10.3847/1538-4357/ac4418
Putman, M. E., Zheng, Y., Price-Whelan, A. M., et al. 2021, ApJ, 913, 53, doi: 10.3847/1538-4357/abe391
Rey, M. P., Pontzen, A., Agertz, O., et al. 2020, MNRAS, 497, 1508, doi: 10.1093/mnras/staa1640
Rhode, K. L., Salzer, J. J., Haurberg, N. C., et al. 2013, AJ, 145, 149, doi: 10.1088/0004-6256/145/6/149
Ricotti, M., & Gnedin, N. Y. 2005, ApJ, 629, 259, doi: 10.1086/431415
Rodriguez Wimberly, M. K., Cooper, M. C., Fillingham, S. P., et al. 2019, MNRAS, 483, 4031, doi: 10.1093/mnras/sty3357
Sacchi, E., Richstein, H., Kallivayalil, N., et al. 2021, ApJL, 920, L19, doi: 10.3847/2041-8213/ac2aa3
Samuel, J., Wetzel, A., Chapman, S., et al. 2020, arXiv e-prints, arXiv:2010.08571. https://arxiv.org/abs/2010.08571
Sand, D. J., Olszewski, E. W., Willman, B., et al. 2009, ApJ, 704, 898, doi: 10.1088/0004-637X/704/2/898
Sand, D. J., Spekkens, K., Crnojević, D., et al. 2015a, ApJL, 812, L13, doi: 10.1088/2041-8205/812/1/L13
Sand, D. J., Strader, J., Willman, B., et al. 2012, ApJ, 756, 79, doi: 10.1088/0004-637X/756/1/79
Sand, D. J., Crnojević, D., Strader, J., et al. 2014, ApJL, 793, L7, doi: 10.1088/2041-8205/793/1/L7
Sand, D. J., Crnojević, D., Bennet, P., et al. 2015b, ApJ, 806, 95, doi: 10.1088/0004-637X/806/1/95
Saviane, I., Held, E. V., & Piotto, G. 1996, A&A, 315, 40. https://arxiv.org/abs/astro-ph/9601165
Sawala, T., Frenk, C. S., Fattahi, A., et al. 2016, MNRAS, 457, 1931, doi: 10.1093/mnras/stw145
Schlafly, E. F., & Finkbeiner, D. P. 2011, ApJ, 737, 103, doi: 10.1088/0004-637X/737/2/103
Simon, J. D. 2019, ARA&A, 57, 375, doi: 10.1146/annurev-astro-091918-104453
Simon, J. D., Brown, T. M., Drlica-Wagner, A., et al. 2021, ApJ, 908, 18, doi: 10.3847/1538-4357/abd31b
Skillman, E. D., Côté, S., & Miller, B. W. 2003, AJ, 125, 593, doi: 10.1086/345964
Smercina, A., Bell, E. F., Price, P. A., et al. 2018, ApJ, 863, 152, doi: 10.3847/1538-4357/aad2d6
Smercina, A., Bell, E. F., Samuel, J., & D'Souza, R. 2021, arXiv e-prints, arXiv:2107.04591. https://arxiv.org/abs/2107.04591
Stetson, P. B. 1987, PASP, 99, 191, doi: 10.1086/131977
—. 1994, PASP, 106, 250, doi: 10.1086/133378
Tarumi, Y., Yoshida, N., & Frebel, A. 2021, ApJL, 914, L10, doi: 10.3847/2041-8213/ac024e
Teyssier, M., Johnston, K. V., & Kuhlen, M. 2012, MNRAS, 426, 1808, doi: 10.1111/j.1365-2966.2012.21793.x
The Astropy Collaboration, Price-Whelan, A. M., Sipőcz, B. M., et al. 2018, ArXiv e-prints. https://arxiv.org/abs/1801.02634
Tollerud, E. J., Geha, M. C., Grcevich, J., Putman, M. E., & Stern, D. 2015, ApJL, 798, L21, doi: 10.1088/2041-8205/798/1/L21
Tollerud, E. J., Geha, M. C., Grcevich, J., et al. 2016, ApJ, 827, 89, doi: 10.3847/0004-637X/827/2/89
Tollerud, E. J., & Peek, J. E. G. 2018, ApJ, 857, 45, doi: 10.3847/1538-4357/aab3e4
Toloba, E., Sand, D. J., Spekkens, K., et al. 2016, ApJL, 816, L5, doi: 10.3847/2041-8205/816/1/L5
Walsh, S. M., Willman, B., Sand, D., et al. 2008, ApJ, 688, 245, doi: 10.1086/592076
Weisz, D., & Boylan-Kolchin, M. 2019, BAAS, 51, 1. https://arxiv.org/abs/1901.07571
Weisz, D. R., Dolphin, A. E., Skillman, E. D., et al. 2014a, ApJ, 789, 147, doi: 10.1088/0004-637X/789/2/147
Weisz, D. R., Dalcanton, J. J., Williams, B. F., et al. 2011, ApJ, 739, 5, doi: 10.1088/0004-637X/739/1/5
Weisz, D. R., Zucker, D. B., Dolphin, A. E., et al. 2012, ApJ, 748, 88, doi: 10.1088/0004-637X/748/2/88
Weisz, D. R., Skillman, E. D., Hidalgo, S. L., et al. 2014b, ApJ, 789, 24, doi: 10.1088/0004-637X/789/1/24
Weisz, D. R., Dolphin, A. E., Martin, N. F., et al. 2019, MNRAS, 489, 763, doi: 10.1093/mnras/stz1984
Westmeier, T. 2018, MNRAS, 474, 289, doi: 10.1093/mnras/stx2757
Wetzel, A. R., Hopkins, P. F., Kim, J.-h., et al. 2016, ApJL, 827, L23, doi: 10.3847/2041-8205/827/2/L23

This figure "TucX_image.png" is available in "png" format from:

http://arxiv.org/ps/2205.09129v2